Applied Biological Research 24(3): 335-344; (2022)
DOI: 10.5958/0974-4517.2022.00040.4

FACILE SYNTHESIS AND SIZE DISTRIBUTION ANALYSIS OF SILVER NANOPARTICLES OF FUNGUS *Penicillium crustosum*, ISOLATED FROM *Taxus baccata* Linn.

Ankush Sharma* and Anand Sagar

Department of Biosciences, Himachal Pradesh University, Summerhill, Shimla -171 005, Himachal Pradesh (India)
*e-mail: *theankushsharma@gmail.com*

(Received 24 April, 2022; accepted 6 August, 2022)

ABSTRACT

The present study was aimed at the synthesis and size distribution analysis of silver nanoparticles (AgNPs), from a fungal endophyte *Penicillium crustosum*. The fungus was isolated from the needles of *Taxus baccata* Linn. and identified as *Penicillium crustosum* by molecular characterization. The fungal extract of *P. crustosum* was subjected to the synthesis of AgNPs. UV-vis-spectroscopy confirmed the formation of AgNPs by forming the specific peaks at 390-450 nm. The lyophilized AgNPs were subjected to size distribution analysis using tools like X-ray diffraction, energy dispersive spectroscopy (EDS), field emission scanning electron microscopy (FEG-SEM), and high-resolution transmission electron microscopy (HRTEM). The average crystalline size of AgNPs was calculated by Debye-Scherrer's formula which showed AgNPs of 36.93 nm. These findings substantiated the results of FEG-SEM and HRTEM, where the average size was below 50 nm. Dynamic light scattering results showed Z-average of AgNPs as 352.0 rnm with 0.982 PdI. Zeta potential was -19.1 mV which showed the capacity of formed AgNPs to decline agglomeration. EDS analysis proved that the requisite phase of silver is present in the sample. The present study displayed the potential of *P. crustosum* as reducing agent which converted silver ions into AgNPs in eco-friendly and cost-effective manner.

Keywords: Energy dispersive spectroscopy, HRTEM, *Penicillium crustosum*, silver nanoparticles, *Taxus baccata*

INTRODUCTION

Nanotechnology is presently playing a crucial role in the modern world specifically especially in drug delivery, as antibacterial agents, food industry, and as anti-cancerous agents (Mukherjee *et al.,* 2001; Chernousova and Epple, 2010; Li *et al.*, 2010; Gurunathan *et al.*, 2015). The specific properties such as optical, electronic, and magnetic properties held by nanoparticles are increasing their utility day by day (Khan *et al.,* 2019). Among other metallic nanoparticles, silver nanoparticles (AgNPs) are promising due to their high biocompatibility (Saravanakumar *et al.,* 2021). The beneficial properties of AgNPs such as high stability, high solubility, and their broad spectrum of biological activities are increasing its priority (Li *et al.,* 2010). The green synthesis of AgNPs using plants, fungi, and bacteria is quite cost-effective and less toxic. The utilization of waste materials and requirement of lesser amount of harmful chemicals make this process quite cost-effective (Sharma *et al*., 2019). There are many reports on the utilization of fungi as synthesizers of metallic nanoparticles (Bhainsa and D'souza, 2006; Mukherjee *et al.,* 2008; Afify *et al.,* 2017; Shaheen *et al.,* 2019). Also, there is a quite interesting relationship between the bioactivity of plant material and its fungal endophytes. The

bioactivity of plant material may be due to the secondary metabolites secreted by the endophytes that reside in plant. The secondary metabolites are generally mimicked by fungal species present in a specific host, which means the reduction process of metallic solution and nanoparticles synthesis is very similar to a certain extent both in endophyte and host plant (Kusari *et al.*, 2008; Kusari and Spiteller, 2012). These biologically synthesized AgNPs hold a characteristic property of acting on a vast area and show high effectiveness as compared to the plant or fungal extract. The size of the biosynthesized AgNPs plays a vital role in the efficacy of AgNPs (Dong *et al*., 2019).

Taxus baccata has previously been used to isolate the endophytic fungi, which were used to synthesize metallic nanoparticles (Sharma *et al.*, 2017; Farsi and Farokhi, 2018; Sharma *et al.*, 2022). The fungus *Penicillium* sp., isolated from *Glycosmis mauritiana*, has reportedly been found effective in producing AgNPs which shows good quality antioxidant, antimicrobial, anti-inflammatory and tyrokinase inhibitory activities (Govindappa *et al.*, 2016). The reports reveal light-induced extra-cellular synthesis of AgNPs by using algicolous endophytic fungus *Penicillium polonicum* ARA 10, isolated from marine green alga *Chetomorpha antennina* (Neethu *et al.*, 2018). The size and morphology of AgNP play a crucial role in drug delivery and effectiveness. X-ray diffraction (XRD) is an effective tool that helps in the determination of size and shape of synthesized nanoparticles. The presence of specific and sharp peaks substantiates the formation of crystalline nanoparticles. The average size of AGNPs was determined by Debye-Scherrer's formula. EDS is another tool where peaks at specific points confirm the synthesis of AgNPs. Atomic percent and weight percent in a sample are determined by EDS. The present study was aimed to isolate *Penicillium* sp. from the needles of *T. baccata*, synthesize AgNPs and confirm its size by XRD and EDS. The study illustrates the methods for obtaining effective size of biosynthesized AgNPs which may help in understanding the efficacy of AgNPs.

MATERIALS AND METHODS

All the experiments were conducted at room temperature (27°C). However, for culturing of fungal isolates BOD incubator was used. The analytical chemicals such as $AgNO_3$ were purchased from Merck, India. Glasswares were procured from Borosil and Harco, India.

Collection of plant material

For collection of plant tissues, the needles of *Taxus baccata* was selected from Churdhar region (between Shimla and Sirmour districts) of Himachal Pradesh, India. Churdhar peak (3647 m) is the highest peak in outer Himalayas. Churdhar lies 30°52' N and 77°32' E at an elevation of 3647 m amsl with altitude 2000-3650 m, rainfall 1500 mm and temperature 5 to 20°C. The plants were identified by Prof. M.K. Seth, Department of Biosciences, Himachal Pradesh University, Summerhill, Shimla. The plant material (needles) was brought to the laboratory in sterilized plastic bags.

Isolation of endophytic fungi

The plant needles were cut into small pieces with a sterilized blade and placed in petri-plates containing potato dextrose agar (PDA) supplemented with 100 mg L^{-1} streptomycin (Himedia). The petri-plates were incubated at 28±2˚C or kept at room temperature. The isolated fungus was sub-cultured until a pure culture was obtained. After the incubation of fungus for 5-7 days, the fungal mycelium was transferred to Petri-plates containing PDA. After 7 days, the growth pattern and colour of mycelium and spores were observed. Slides of fungus were prepared containing mycelium, hyphae and spores and observed under Lieca microscope. After preliminary identification, the identity of isolated fungus was got confirmed by National Fungal Culture Collection of India (NFCCI), Agharkar Research Institute (ARI), Pune, India.

The molecular characterization of isolated fungus was carried out by PCR using ITS4 and ITS5 as primer pair (Sharma *et al.*, 2022). The genomic DNA was isolated form from the culture. The ITS-

rDNA partial gene was successfully amplified using ITS and ITS5. The sequencing of PCR was done with ABI-BigDye® Terminator v 3.1 cycle sequencing kit. The raw sequence obtained from ABI 3100 automated DNA sequencer was manually edited for inconsistency. The sequence data was aligned with publicly available sequences and analyzed. All these processes were carried out at NFCCI, ARI, Pune (India).

Synthesis of silver nanoparticles from fungus

For AgNP synthesis from *P. crustosum*, the method of Sandhu *et al.* (2017) was followed with slight modifications. An aqueous solution of silver nitrate (80 mL; 2 mM) was mixed with 20 mL fungal extract and incubated at room temperature. For determination of successful synthesis of AgNPs, UV-visible spectrophotometry (Shimadzu) was done by measuring the absorbance of solution at different time intervals (1, 12, 24, 48, 72, and 96 h) at 300-700 nm. After confirmation of AgNP formation, the sample was centrifuged repeatedly at 10,000 rpm for 15 min which was followed by re-dispersion of the formed pellet in deionized water. The pellet was lyophilized to obtain dry powder. The size distribution analysis was performed by using X-ray diffraction (XRD), dynamic light scattering, FEG-SEM (field emission gun surface electron microscopy). HRTEM (high-resolution transmission electron microscopy) and EDS. XRD analysis was used to determine the morphology and crystalline nature of AgNPs/INPs in a wide range of Bragg angles 2θ at scanning rate 30-80 at 0.041 min^{-1} with a time constant of 2s. XRD is a quick analytical tool used to identify the phases of a crystalline material which also provides the information about the unit cell dimensions. When the sample interacts with the incident rays it produces a constructive interference only when Bragg's law ($n\lambda = 2d \sin \theta$) is satisfied. Bragg's law relates the wavelength of electromagnetic radiation to the diffraction angle and lattice spacing in a crystalline sample. In XRD, the sample is scanned through a wide range of 2θ angles where the powdered sample is oriented randomly resulting in various diffraction directions of lattice. Every mineral has a set of unique d-spacings. The diffraction peaks are converted to d-spacings which help in identifying the mineral (Cullity, 1978). The results were compared with the standard reference patterns available in ICDD (International Centre of Diffraction Data). The particle size is also calculated in XRD by using Debye-Scherrer's equation:

$$D = 0.9 \lambda/\beta \cos \theta$$

Here 'λ' is the wave length of X-ray (0.15416 nm) and 'β' is the full width half maximum (FWHM), 'θ' is the diffraction angle and 'D' is particle diameter size.

DLS and ZPA (Zeta potential analysis) measurements are the tools which reveal the appropriate particle size and surface charge of nanoparticles. Dispersed nanoparticles scatter incident light proportional to the 6^{th} power of their radii. The results of DLS depend on the variables like solvent viscosity, temperature and refractive index of material. Nanoparticles have an inherent property of agglomeration (Liu *et al*., 2011). More the concentration of material, bigger is agglomeration; and the results obtained are diffused. For good quality results in DLS, dilute concentrations are preferred (Zhou *et al*., 2015). DLS measures a larger number of particles thus giving a more robust data on size distribution and PDI (poly dispersity index). PDI has various values when a sample is analysed in DLS. According to International Standards Organizations, the sample having PDI value < 0.05 are generally monodisperse; however, the values > 0.7 are generally polydisperse or broad sized. The size was analyzed using dynamic light scattering analysis (DLS-Malvern Zetasizer®). ZPA reflects the potential difference between electric double layer (EDL) of electrophoretically mobile particles and the layer of dispersant around them at the slipping plane. Ionic strength compressed EDL and decreased zeta potential. Concentrations of particles play major role in ZPA. Zeta potential value of ± 0-10 mV is considered highly unstable, while the value of ±10-20 mV is relatively stable and >±30 mV is highly stable (Patel *et al*., 2011).

For surface morphological studies, FEGSEM technique was used. The morphological character analyses were carried out using a scanning electronic microscope (Hitachi S-4500 SEM). Thin film samples were prepared on a carbon coated copper grid by dropping a small amount of sample on the grid. The extra solution was removed using a blotting paper, and the films were allowed to dry by

subjecting under a mercury lamp for 5 min. For elemental analysis, FEGSEM-EDS was used. In EDS, single sensor large area (50 mm^2) silicon drift detector sensor was used with count rates > 500,000 cps, throughput > 200,000 cps and resolution @ 127eV @ MnKα. The EDS analyzed elements from Be to Pu, where qualitative and semi-quantitative elemental analysis was done. Results were presented as spectral imaging.

For analysis of shape and size of synthesized nanoparticles, the AgNP powder was suspended in ethanol for high-resolution transmission electron microscopy (HRTEM). The presence of specific metallic groups was found with the help of HRTEM-EDS (energy-dispersive X-ray spectroscopy).

RESULTS AND DISCUSSION

The morphological identification of fungus was done at ARI, Pune, India, wherein the fungus with code TL6 was confirmed to be *Penicillium crustosum*. The fungus was a blue-green or green grey mold having specifically biseriate conidiophores on which phialides produced asexual spores. The colonies were fasciculate to crustose. The colour of colonies was dull green with white thin edge. The colour observed on the reverse side of Petri-plate was creamish. Terverticillate conidiophores (Fig. 1a,b) were arranged on cylindrical phialides carrying globose/sub-globose and smooth-walled conidia (Demjanova *et al.*, 2021). Molecular identification of fungus was done by ITS-rDNA partial gene amplification using ITS4 and ITS5. The sequencing PCR was set up with ABI-BigDye®Terminatorv-3. It was aligned with publicly available sequences and analysed to confirm the identity. *P. crustosum* was mass cultured in potato dextrose broth (PDB). The mycelia was weighed, filtered, and used for the synthesis of silver nanoparticles (AgNPs).

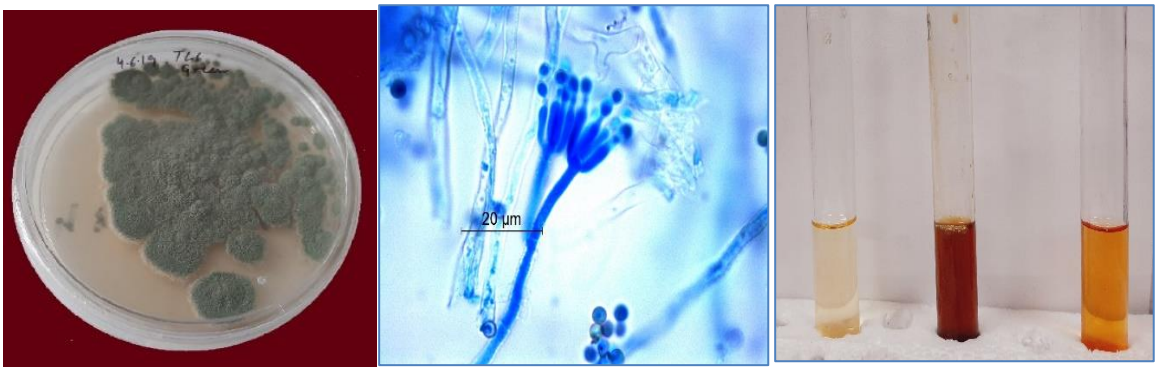

(a) (b) (c)

Fig. 1: a) *Penicillium crustosum* grown on solid agar medium, b) *P. crustosum* microscopic image showing hyphae and spores; c) Colour change in reaction mixture after 24, 48 and 72 h

The fungal strain TL6 showed 100% sequence similarity with *Penicillium crustosum*. Sequence analysis with NCBI Accession No. MH427070.1, *Penicillium crustosum* strain OR6 resulted in following alignment statistics. Alignment statistics: Querry length - 542, Score - 978 bits (1084), Expect - 0.0, Identities - 542/542 (100%), Gaps - 0/542 (0%), Strand - Plus/Plus.

The top five hits upon BLASTn analysis were:

Gene bank Accession No.	The strains of *Penicillium crustosum*	Max score	Query cover	Query coverage	E-value	Identity (%)	Reference
MH427070.1	strain OR6	978	978	100%	0.0	100	Altschul, *et al.* (1990)
MH427064.1	strain CO5	978	978	100%	0.0	100	
MH427056.1	strain AP1	978	978	100%	0.0	100	
MN017794.1	strain M1	978	978	100%	0.0	100	
MN007134.1	strain M12	978	978	100%	0.0	100	

The alignment statistics are as follows:

Query 1	TGAGGGCCCTCTGGGTCCAACCTCCCACCCGTGTTTATTTTACCTTGTTGCTTc g g c g g g	60
Sbjct 27	TGAGGGCCCTCTGGGTCCAACCTCCCACCCGTGTTTATTTTACCTTGTTGCTTCGGCGGG	86
Query 61	c c c g c c t t a a c t g g c c g c c g g g g g g g c t t ac g c c c c c g g g c c c g c g c c c g c c gAAGACACC	120
Sbjct 87	CCCGCCTTAACTGGCCGCCGGGGGGCTTACGCCCCCGGGCCCGCGCCCGCCGAAGACACC	146
Query 121	CTCGAACTCTGTCTGAAGATTGAAGTCTGAGTGAAAATATAAATTATTTAAAACTTTCAA	180
Sbjct 147	CTCGAACTCTGTCTGAAGATTGAAGTCTGAGTGAAAATATAAATTATTTAAAACTTTCAA	206
Query 181	CAACGGATCTCTTGGTTCCGGCATCGATGAAGAACGCAGCGAAATGCGATACGTAATGTG	240
Sbjct 207	CAACGGATCTCTTGGTTCCGGCATCGATGAAGAACGCAGCGAAATGCGATACGTAATGTG	266
Query 241	AATTGCAAATTCAGTGAATCATCGAGTCTTTGAACGCACATTGCGCCCCCTGGTATTCCG	300
Sbjct 267	AATTGCAAATTCAGTGAATCATCGAGTCTTTGAACGCACATTGCGCCCCCTGGTATTCCG	326
Query 301	GGGGGCATGCCTGTCCGAGCGTCATTGCTGCCCTCAAGCCCGGCTTGTGTGTTGGGCCCC	360
Sbjct 327	GGGGGCATGCCTGTCCGAGCGTCATTGCTGCCCTCAAGCCCGGCTTGTGTGTTGGGCCCC	386
Query 361	GTCCCCCGATCTCCGGGGGACGGGCCCGAAAGGCAGCGGCGGCACCGCGTCCGGTCCTCG	420
Sbjct 387	GTCCCCCGATCTCCGGGGGACGGGCCCGAAAGGCAGCGGCGGCACCGCGTCCGGTCCTCG	446
Query 421	AGCGTATGGGGCTTTGTCACCCGCTCTGTAGGCCCGGCCGGCGCTTGCCGATCAACCCAA	480
Sbjct 447	AGCGTATGGGGCTTTGTCACCCGCTCTGTAGGCCCGGCCGGCGCTTGCCGATCAACCCAA	506
Query 481	ATTTTTATCCAGGTTGACCTCGGATCAGGTAGGGATACCCGCTGAACTTAAGCATATCAA	540
Sbjct 507	ATTTTTATCCAGGTTGACCTCGGATCAGGTAGGGATACCCGCTGAACTTAAGCATATCAA	566
Query 541	TA 542	
Sbjct	TA 568	

In present study, the endophytic fungus *Penicillium crustosum*, isolated from *Taxus baccata*, was used for the synthesis of silver nanoparticles (AgNPs). The formation of AgNP was confirmed first by observing the colour change in solution, and then by using UV-vis spectroscopy. Sharp peaks were observed at 370-450 nm (Fig. 2). These peaks were formed due to surface Plasmon resonance of myco-synthesized AgNPs (Nair and Pradeep, 2003; Sathiyaseelan *et al.*, 2020).

DLS (dynamic light scattering) measurements were performed to assess the size distribution of AgNPs. For PcAgNPs the Z-average was 352 r.nm and 0.982 PdI. The zeta potential analysis showed a high negative value (-19.1 mV for PcAgNPs) which confirmed the tendency of nano-particles to decline agglomeration (Shaligram *et al.*, 2009; Suresh *et al.*, 2011). Crystalline nature of AgNPs was obtained in X-ray diffraction analysis (Fig. 3) where the XRD analysis exhibited diffraction peaks corresponding to [111], [200], [220] and [311] appearing at 2θ value (Shaligram *et al.*, 2009). These results confirmed the presence of AgNPs as crystalline fcc which is as per the database of ICDD File No. 04-0783. For calculation of average crystalline size of synthesized AgNPs Debye-Scherrer's

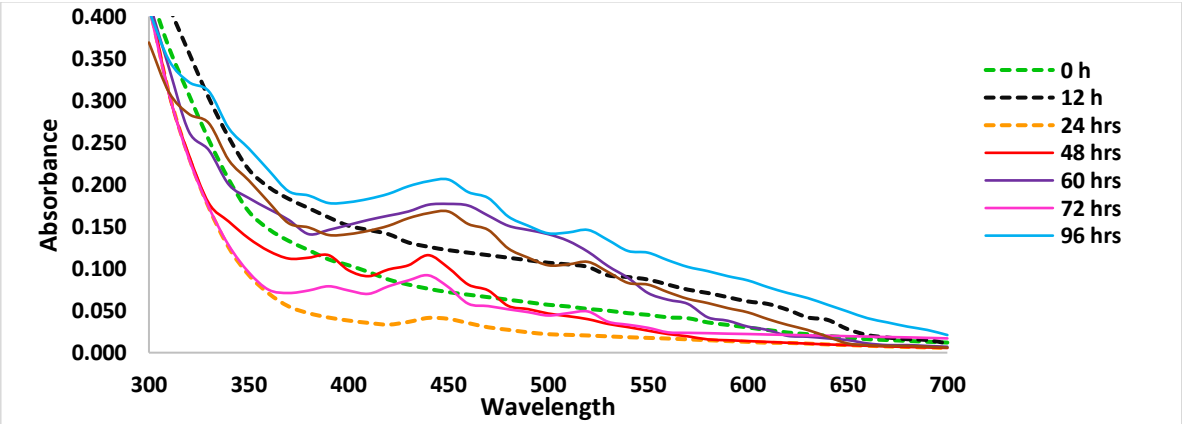

Fig. 2: UV-vis spectroscopy of fungal extract of *P. crustosum*

formula was used:

$$D = 0.9 \lambda/\beta \cos \Theta$$

Here '**λ**' is the wavelength of X-ray (0.15416 nm) and '**β**' is the full width half maximum (FWHM), '**Θ**' is the diffraction angle and 'D' is particle diameter size.

The average size according to Debye-Scherrer's equation was found to be 34.93 nm. The sharpness of peaks suggests that the particles formed were of nanosize. The additional peaks observed in XRD analysis suggested the occurrence of a bio-organic phased on the surface of synthesized AgNPs, clearly revealing the role of fungal extract in the reduction of silver ions. The results are in line with the previous XRD reports of biosynthesized AgNPs (Brumfitt *et al.*, 1990; Balaji *et al.*, 2009; Kotakadi *et al.*, 2016). Indexing was done and the data is represented in Table 1.

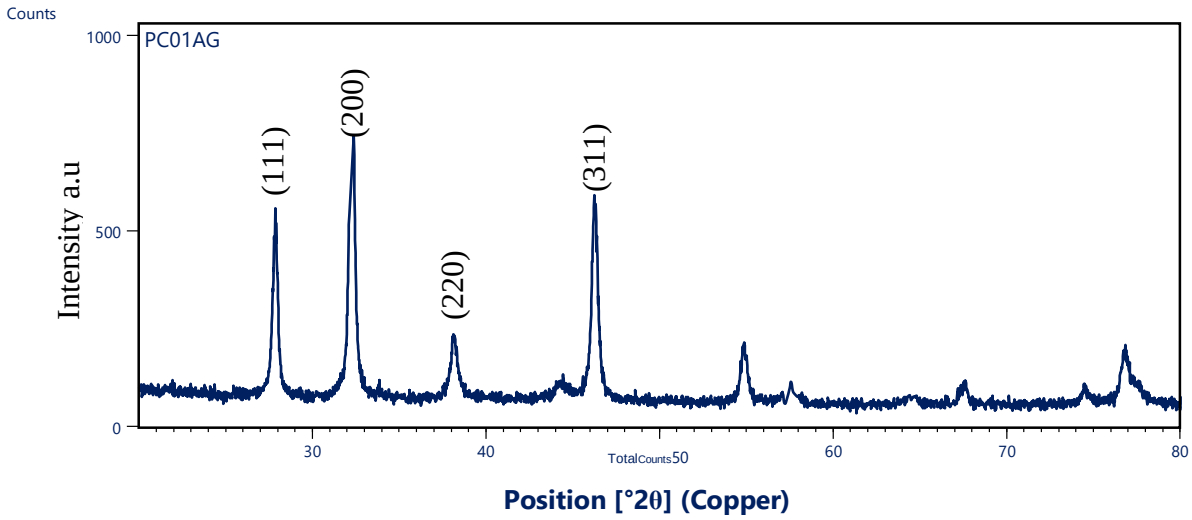

Fig. 3: X-ray diffraction analysis of AgNPs synthesized from *P. crustosum*

Table 1: The grain size of silver nanoparticles synthesized from *P. crustosum*

POS.˚2Θ	˚Θ	˚Θ to radians	Cos radians	FWHM ˚2Θ	FWHM ˚Θ	FWHM to radians ß	Size (nm)	Average size (nm)
32.2507	16.1253	0.28144045	0.96065636	0.3239	0.1619	0.00282656	47.1240000	34.926948
46.2362	23.1181	0.40348696	0.91969751	0.3634	0.1817	0.00317126	40.2110227	
54.8248	27.4124	0.47843663	0.88771576	0.3787	0.1893	0.00330478	37.2446296	
67.4676	33.7338	0.58876587	0.83162666	0.4688	0.2344	0.00409105	28.1855058	
76.8165	38.4082	0.67035042	0.78360401	0.5693	0.2846	0.00496808	21.8695827	

The results thus obtained by XRD were substantiated by the observations of FEG-SEM and HRTEM. In FEG-SEM (Fig. 4a), the AgNPS showed a variety of shapes and size. Clump formation was also observed. The results are in accordance with the findings of Jyoti *et al.* (2016). HRTEM analysis (Fig. 4b) showed that the myco-synthesized AgNPs had spherical shape with a diameter in the range of 20 to 50 nm.

HRTEM-EDS analysis (Fig. 5) confirmed the presence of 93.3% Ag by weight percent and 61.97% by atomic percent. Synthesized AgNPs were confirmed by the strong peak at 3.0 keV in EDS (Fig. 7).

During EDS some other elements like carbon, nitrogen and oxygen were also found along with silver (Table 2). The results showed similarities with the previous results (Chen *et al.*, 2009; Okafor *et al.*, 2013; Lee *et al.*, 2014; Hu *et al.*, 2019) where various endophytic fungal extracts resulted in the synthesis of silver nanoparticles.

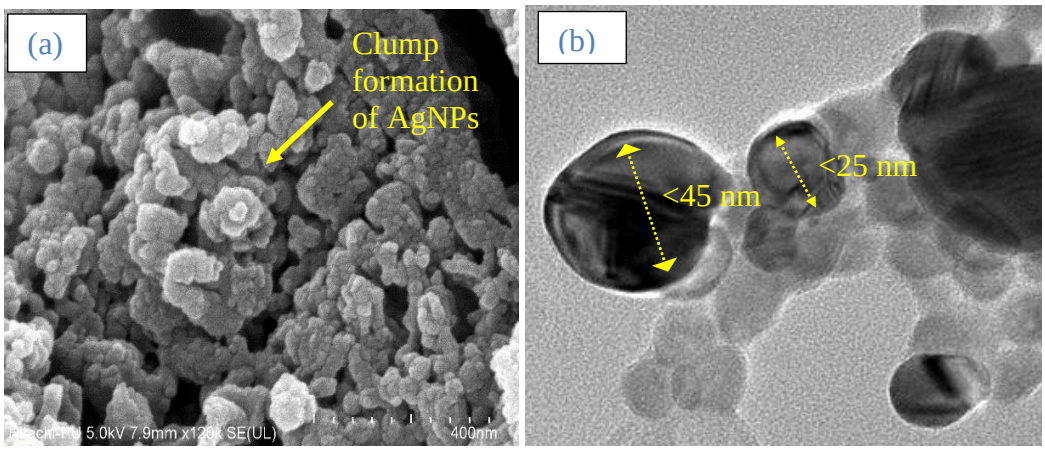

Fig. 4: AGNPs synthesized from *P. crustosum* a) FEG-SEM image, b) HRTEM image

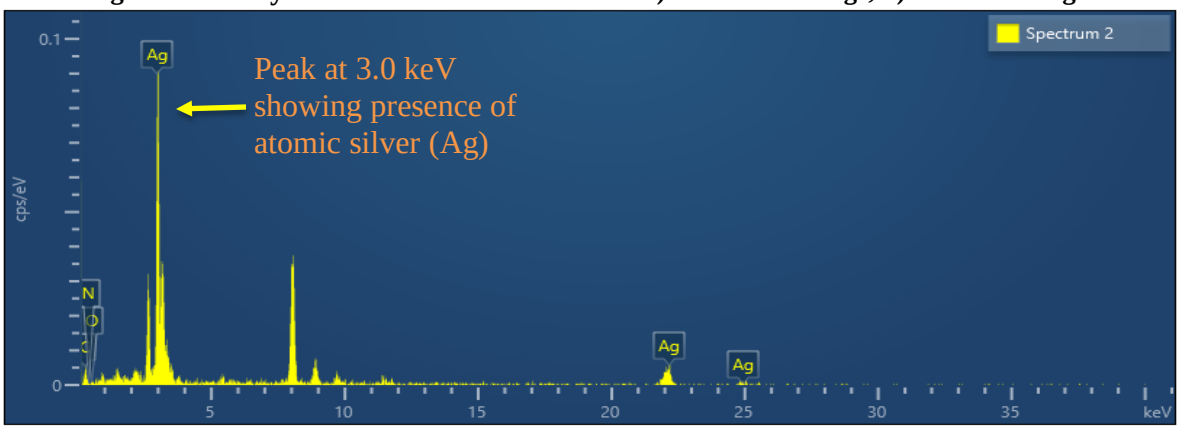

Fig. 5: EDS (energy dispersive spectroscopy) of synthesized from *P. crustosum*

Table 2*:* Weight % and atomic % in AgNP's synthesized from *P. crustosum*

Elements	Line type	Weight (%)	Atomic (%)*
C	K series	5.14	30.65
N	K series	0.83	4.26
O	K series	0.70	3.12
Ag	K series	93.33	61.97
Total		100	100

*Atomic (%) is the number of atoms of an element, at that weight percentage, divided by the total number of atoms in the sample multiplied by 100.

Conclusion: The process of mycosynthesis of silver nanoparticles is a low-cost, least toxic and prominent way to produce AgNPs at room temperature. The fungus *Penicillium crustosum* was isolated from the leaves of *Taxus baccata*. The fungal extract was used as a reducing and stabilizing agent. The XRD results showed the formation of crystalline AgNPs having the average size of ~34.93 nm as per Debye-Scherrer's formula. The zeta potential analysis showed a negative value confirming the decline in agglomeration of AgNPs. XRD results were substantiated by HRTEM. The EDS analysis confirmed the presence of required phase of silver in the sample. Further studies are required to explain the other biological properties like anti-microbial, antioxidant, and anti-cancerous properties of these synthesized AgNPs.

Conflict of interest: The authors declare that they have no conflict of interest.

Funding: No funding/grant was received for this research work.

REFERENCES

Afify, T.A., Saleh, H.H. and Ali, Z.I. 2017. Structural and morphological study of gamma-irradiation synthesized silver nanoparticles. *Polymer Composites*, **38**(12): 2687-2694.

Altschul, S.F., Gish, W., Miller, W., Myers, E.W. and Lipman, D.J. 1990. Basic local alignment search tool. *Journal of Molecular Biology*, **215**(3): 403-410.

Balaji, D.S., Basavaraja, S., Deshpande, R., Mahesh, D.B., Prabhakar, B.K. and Venkataraman, A. 2009. Extracellular biosynthesis of functionalized silver nanoparticles by strains of *Cladosporium cladosporioides* fungus. *Colloids and Surfaces B: Biointerfaces*, **68**(1): 88-92.

Bhainsa, K.C. and D'souza, S.F. 2006. Extracellular biosynthesis of silver nanoparticles using the fungus *Aspergillus fumigatus*. *Colloids and Surfaces B: Biointerfaces*, **47**(2): 160-164.

Brumfitt, W., Hamilton-Miller, J.M. and Franklin, I. 1990. Antibiotic activity of natural products: 1. Propolis. *Microbios*, **62**(250): 19-22.

Chen, J.C., Lin, Z.H. and Ma, X.X. 2003. Evidence of the production of silver nanoparticles via pretreatment of *Phoma* sp. 3.2883 with silver nitrate. *Letters in Applied Microbiology*, **37**(2): 105-108.

Chernousova, S. and Epple, M. 2013. Silver as antibacterial agent: Ion, nanoparticle, and metal. *Angewandte Chemie International Edition*, **52**(6): 1636-1653.

Cullity, B.D. 1978. *Elements of X-ray Diffraction.* (1st edn.). Addison.Wesley Publishing Co., USA.

Demjanová, S., Jevinová, P., Pipová, M. and Regecová, I. 2021. Identification of *Penicillium verrucosum*, *Penicillium commune* and *Penicillium crustosum* isolated from chicken eggs. *Processes*, **9**(1): 53. [*https://doi.org/10.3390/pr9010053*].

Dong, Y., Zhu, H., Shen, Y., Zhang, W. and Zhang, L. 2019. Antibacterial activity of silver nanoparticles of different particle size against *Vibrio* Natriegens. *PloS one*, **14**(9): e0222322. [*https://doi.org/10.1371/journal.pone.0222322*].

Farsi, M. and Farokhi, S. 2018. Biosynthesis of antibacterial silver nanoparticles by endophytic fungus *Nemania* sp. isolated from *Taxus baccata* L. (Iranian yew). *Zahedan Journal of Research in Medical Sciences*, **20**(6): e57916. [*https://dx.doi.org/10.5812/zjrms.57916*].

Govindappa, M., Farheen, H., Chandrappa, C.P., Rai, R.V. and Raghavendra, V.B. 2016. Mycosynthesis of silver nanoparticles using extract of endophytic fungi, *Penicillium* species of *Glycosmis mauritiana,* and its antioxidant, antimicrobial, anti-inflammatory and tyrokinase inhibitory activity. *Advances in Natural Sciences: Nanoscience and Nanotechnology*, **7**(3): 035014. [*https://dx.doi.org/10.1088/2043-6262/7/7/03514*].

Gurunathan, S., Park, J.H., Han, J.W. and Kim, J.H. 2015. Comparative assessment of the apoptotic potential of silver nanoparticles synthesized by *Bacillus tequilensis* and *Calocybe indica* in MDA-MB-231 human breast cancer cells: targeting p53 for anticancer therapy. *International Journal of Nanomedicine*, **10**: 4203. [*https://doi.org/10.2147/ijn.s83953*].

Hu, X., Kandasamy Saravanakumar, T.J. and Wang, M.H., 2019. Mycosynthesis, characterization, anticancer and antibacterial activity of silver nanoparticles from endophytic fungus *Talaromyces purpureogenus*. *International Journal of Nanomedicine*, **14**: p. 3427. [*https://doi.org/10.2147/ijn.s200817*].

Jyoti, K., Baunthiyal, M. and Singh, A. 2016. Characterization of silver nanoparticles synthesized using *Urtica dioica* Linn. leaves and their synergistic effects with antibiotics. *Journal of Radiation Research and Applied Sciences*, **9**(3): 217-227.

Khan, I., Saeed, K. and Khan, I., 2019. Nanoparticles: Properties, applications and toxicities. *Arabian Journal of Chemistry*, **12**(7): 908-931.

Kotakadi, V.S., Gaddam, S.A., Venkata, S.K., Sarma, P.V.G.K. and Sai Gopal, D.V.R. 2016. Bio-fabrication and spectral characterization of silver nanoparticles and their cytotoxic studies on human CD34 +ve stem cells. *Biotech*, **6**(2): 216. [*https://doi.org/10.1007/s13205-016-0532-5*].

Kusari, S., Lamshöft, M., Zühlke, S. and Spiteller, M. 2008. An endophytic fungus from *Hypericum perforatum* that produces hypericin. *Journal of Natural Products*, **71**(2): 159-162.

Kusari, S., Lamshöft, M., Zühlke, S. and Spiteller, M. 2008. An endophytic fungus from *Hypericum perforatum* that produces hypericin. *Journal of Natural Products*, **71**(2): 159-162.

Lee, W., Kim, K.J. and Lee, D.G. 2014. A novel mechanism for the antibacterial effect of silver nanoparticles on *Escherichia coli*. *Biometals*, **27**(6): 1191-1201.

Li, W.R., Xie, X.B., Shi, Q.S., Zeng, H.Y., You-Sheng, O.Y. and Chen, Y.B. 2010. Antibacterial activity and mechanism of silver nanoparticles on *Escherichia coli*. *Applied Microbiology and Biotechnology*, **85**(4): 1115-1122.

Liu, H.H., Surawanvijit, S., Rallo, R., Orkoulas, G. and Cohen, Y. 2011. Analysis of nanoparticle agglomeration in aqueous suspensions via constant-number Monte Carlo simulation. *Environmental Science and Technology*, **45**(21): 9284-9292.

Mukherjee, P, Roy, M., Mandal, B.P., Dey, G.K., Mukherjee, P.K., Ghatak, J., Tyagi, A.K. and Kale, S.P. 2008. Green synthesis of highly stabilized nanocrystalline silver particles by a non-pathogenic and agriculturally important fungus *T. asperellum*. *Nanotechnology*, **19**(7): 075103. [*https://doi.org/10.1088/0957-4484/19/7/075103*].

Mukherjee, P., Ahmad, A., Mandal, D., Senapati, S., Sainkar, S.R., Khan, M.I., Parishcha, R., Ajaykumar, P.V., Alam, M., Kumar, R. and Sastry, M. 2001. Fungus-mediated synthesis of silver nanoparticles and their immobilization in the mycelial matrix: A novel biological approach to nanoparticle synthesis. *Nano Letters*, **1**(10): 515-519.

Nair, A.S. and Pradeep, T. 2003. Halocarbon mineralization and catalytic destruction by metal nanoparticles. *Current Science*, **84**(12): 1560-1564.

Neethu, S., Midhun, S.J., Sunil, M.A., Soumya, S., Radhakrishnan, E.K. and Jyothis, M. 2018. Efficient visible light induced synthesis of silver nanoparticles by *Penicillium polonicum* ARA 10 isolated from *Chetomorpha antennina* and its antibacterial efficacy against *Salmonella enterica* serovar *Typhimurium*. *Journal of Photochemistry and Photobiology B: Biology*, **180**: 175-185.

Okafor, F., Janen, A., Kukhtareva, T., Edwards, V. and Curley, M. 2013. Green synthesis of silver nanoparticles, their characterization, application and antibacterial activity. *International Journal of Environmental Research and Public Health*, **10**(10): 5221-5238.

Patel, V.R. and Agrawal, Y.K. 2011. Nanosuspension: An approach to enhance solubility of drugs. *Journal of Advanced Pharmaceutical Technology and Research*, **2**(2): 81.

Sandhu, S.S., Shukla, H. and Shukla, S. 2017. Biosynthesis of silver nanoparticles by endophytic fungi: Its mechanism, characterization techniques and antimicrobial potential. *African Journal of Biotechnology*, **16**(14): 683-698.

Saravanakumar, K., Sriram, B., Sathiyaseelan, A., Mariadoss, A.V.A., Hu, X., Han, K.S., Vishnupriya, V., Mubarakali, D., and Wang, M.H. 2021. Synthesis, characterization, and cytotoxicity of starch-encapsulated biogenic silver nanoparticle and its improved anti-bacterial activity. *International Journal of Biological Macromolecules*, **182**: 1409-1418.

Sathiyaseelan, A., Saravanakumar, K., Mariadoss, A.V.A. and Wang, M.H., 2020. Biocompatible fungal chitosan encapsulated phytogenic silver nanoparticles enhanced antidiabetic, anti-oxidant and antibacterial activity. *International Journal of Biological Macromolecules*, **153**: 63-71.

Shaheen, M.N., El-hadedy, D.E. and Ali, Z.I. 2019. Medical and microbial applications of controlled shape of silver nanoparticles prepared by ionizing radiation. *BioNanoScience*, **9**(2): 414-422.

Shaligram, N.S., Bule, M., Bhambure, R., Singhal, R.S., Singh, S.K., Szakacs, G. and Pandey, A. 2009. Biosynthesis of silver nanoparticles using aqueous extract from the compactin producing fungal strain. *Process Biochemistry*, **44**(8): 939-943.

Sharma, A., Sagar, A. and Joshi, M. 2017. Diversity of fungi associated with *Taxus baccata* Linn. in different seasons. *Indian Forester*, **143**(4): 380-384.

Sharma, A., Sagar, A., Rana, J. and Rani, R. 2022. Green synthesis of silver nanoparticles and its antibacterial activity using fungus *Talaromyces purpureogenus* isolated from *Taxus baccata* Linn. *Micro- and Nano-Systems Letters*, **10**(1): 1-12.

Sharma, D., Kanchi, S. and Bisetty, K. 2019. Biogenic synthesis of nanoparticles: A review. *Arabian Journal of Chemistry*, **12**(8): 3576-3600.

Suresh, A.K., Doktycz, M.J., Wang, W., Moon, J.W., Gu, B., Meyer III, H.M., Hensley, D.K., Allison, D.P., Phelps, T.J. and Pelletier, D.A. 2011. Monodispersed biocompatible silver sulfide nanoparticles: Facile extracellular biosynthesis using the γ-proteobacterium, *Shewanella oneidensis*. *Acta Biomaterialia*, **7**(12): 4253-4258.

Zhou, C., Qi, W., Lewis, E.N. and Carpenter, J.F. 2015. Concomitant Raman spectroscopy and dynamic light scattering for characterization of therapeutic proteins at high concentrations. *Analytical Biochemistry*, **472**: 7-20.